CHAPTER 4: DESIGN AND SIMULATION OF SILICA-ON-SILICON HYBRID PUMP/SIGNAL MULTIPLEXER FOR APPLICATION IN BROADBAND AMPLIFIER

4.1 Introduction

This chapter describes silica-on-silicon hybrid pump/signal multiplexer for application in broadband amplifiers. Similarly, the uniform symmetric direction coupler plays a significant role in constructing the hybrid pump/signal multiplexer. Hybrid in this case refers to the combination of two or more uniform symmetric direction coupler on the same chip, aimed at achieving broadband amplification.

4.2 Design of Combined 800/1310 nm and 980/1550 nm Uniform Symmetric Direction Couplers

For the purpose of broadening the amplification band for long haul optical fiber communications, a hybrid pump/signal multiplexer is proposed. The characteristics and advantages of these two uniform symmetric direction couplers have been explained in detail Section 3.3 and 3.4, respectively. The two individual direction coupler designs in the previous chapters will be utilized and combined in the broadband amplifier. In the design, the first direction coupler is used to de-multiplex the two signal wavelength (1310 nm and 1550 nm) into the respective amplification medium. In this work, we introduce a design of combined 800/1310 nm and 980/1550 nm uniform symmetric direction couplers which would be integrated into a broadband amplifier as illustrated in Figure 4.1 in order to overcome the increasing demand for bandwidth.

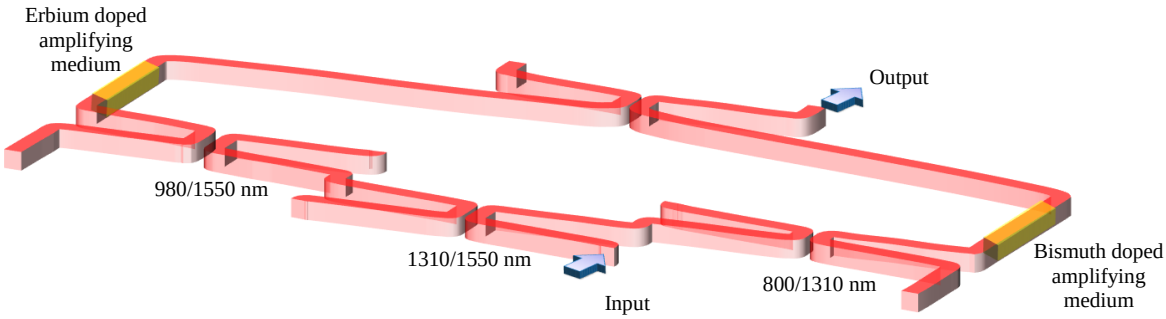

Figure 4.1: A 3D schematic showing the physical layout of the designed broadband amplifier.

This chip consists of two straight waveguide amplification mediums where one is selectively doped with erbium and another is doped with bismuth. However the structure of the amplification medium can be replaced by a spiral topology. The erbium doped amplifying region falls within the 1550 nm window (third telecommunications window), whereas the bismuth doped amplifying region is in the 1310 nm window (second telecommunications window). The typical bandwidth of erbium doped amplifying region is about 70 nm [1]. Meanwhile the amplification bandwidth of bismuth doped is about 300 nm [2]. Subsequently, the two parallel directional couplers serve to multiplex both pump and signal wavelengths into the bismuth doped or erbium doped amplifying regions. As mentioned earlier, the bismuth doped and erbium doped amplifying region was used to amplify the 1310 nm and 1550 nm signals with 800 nm and 980 nm excitation, respectively. A similar device will be used to de-multiplex the two signal wavelengths at the output of the directional coupler. Hence, this design consisting two telecommunication windows is able to achieve higher capacity and bandwidth for Wavelength Division Multiplexing (WDM) systems. This design also fulfills the fabrication limit requirement of silica-on–silicon planar waveguide.

4.3 Structures of Silica-on-Silicon Hybrid Pump/Signal Multiplexer

The 2D physical layout of the silica-on-silicon hybrid pump/signal multiplexer in the broadband amplifier chip is illustrated in Fig.4.2.

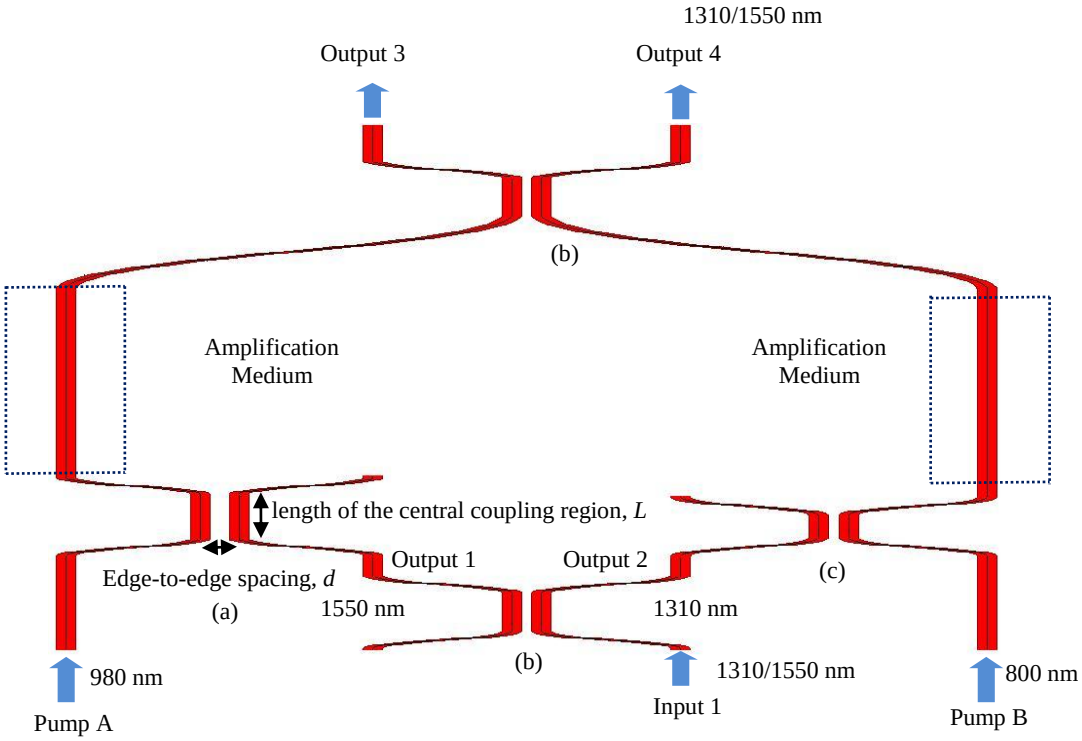

Figure 4.2: A 2D schematic showing the physical layout of the designed broadband amplifier

The amplifier comprises of four uniform symmetric direction couplers with three different combinations of multiplexed/demultiplexed wavelength such as (a) 980/1550 nm, (b) 1310/1550 nm and (c) 800/1310 nm. Each directional coupler consists of two parallel straight waveguides and four diverging waveguide. The diverging waveguides are made up of two arc bends with a curvature radius, *R*. The edge-to-edge spacing between two adjacent waveguides is *d*. The length of the central coupling region is set as *L*.

The rectangular core cross-section of the planar waveguide utilized in the design is 8μm ×8μm. The core of the directional couplers is sandwiched between upper and under cladding layers with slightly lower refractive index. The refractive index of core and cladding are selected to be 1.449 and 1.445 respectively. The directional couplers have a refractive index difference, Δ of 0.28%. In the design, the radius, R_1 of diverging waveguide is fixed at 25 mm. However, the curvature radius, R_2 (input end only) of the second 1310/1550 nm directional coupler is set at 150 mm. It is to connect the amplification region to the second 1310/1550 nm directional coupler. The separation between two inputs or two outputs (channel separation) has to be fixed to be 125 μm apart. Table 4.1 shows the parameters for the silica-on-silicon hybrid pump/signal multiplexer which were utilized for the design.

Table 4.1: Parameters for the silica-on-silicon hybrid pump/signal multiplexer

Parameter	Values
Core dimension	8 μm ×8 μm
Refractive index of core, n_{core}	1.449 at 1550 nm
Refractive index of cladding, $n_{cladding}$	1.445 at 1550 nm
Refractive index difference, Δ	0.28%
curvature radius, R_1	25 mm
curvature radius, R_2	150 mm

The next section provides the simulations results of the silica-on-silicon hybrid pump/signal multiplexer

4.4 Simulation Results of Silica-on-Silicon Hybrid Pump/Signal Multiplexer

The 3D FD-BPM was employed to simulate the light propagation across a waveguide within hybrid pump/signal multiplexer in order to validate the design. The design validation is performed via Rsoft BeamPROP. In the 3D BPM modeling, a step index profile was adopted. To evade incorrect field calculation for the s-bend, the automatic tilt function was utilized for BPM launch and monitor and a full transparent boundary condition was implemented to avoid reflection to the core. Similar to the directional coupler simulation in the previous chapter, the Gaussian mode was chosen for the launch field and the intensity monitor is controlled by launch power. The scalar field was selected and utilized in the latter simulation because from the waveguide parameter as stated earlier, the waveguide is less sensitive to polarization. This is verified through using equation (3.6).

Due to a design that comprises of three different pump/signal multiplexers or de-multiplexers combinations: 980/1550 nm, 800/1310 nm and 1310/1550 nm, the characteristic of each directional coupler are investigated separately. The first and second designs have already been completed in the previous chapter. For the two previous configurations, the edge-to-edge spacing increased to 7.8 μm whereas the length of central coupling region remains as 6200 μm for the 980/1550 nm directional coupler. The waveguide parameters of 800/1310 nm directional coupler design are 4.5 μm as edge-to-edge spacing, d and 3317.5 μm as optimum length of central coupling region, L.

Similiar to work conducted on the two previous directional couplers designs, the investigation into the effect of length of central coupling region, L and edge-to-edge spacing d were carried out for 1310/1550 nm directional coupler. With reference to

Figure 4.2 (b), the 1310 nm and 1550 nm signal wavelengths from the input ports are de-multiplexed to output 1 and output 2, respectively. The intensity of outputs 1 and 2 for the 1310 nm and 1550 nm signal wavelengths were simulated as illustrated in Figure 4.3. The highest normalized output intensity for the 1310 nm and 1550 nm signal wavelengths are 88% and 87%, respectively. In Figure 4.3 (a), the possible optimum parameters for 1310 nm coupling are limited in the region from 3.5 to 4.0 μm of the edge-to-edge spacing and 5000 to 5500 μm of length of central coupling region. Meanwhile, the optimum edge-to-edge separation and optimum length of central coupling region range for 1550 nm coupling is limited in the region similar to the 1310 nm coupling. The optimum parameters are limited in the rectangular box as shown in Figure 4.3 which serves as a rough indication for obtaining optimum parameter.

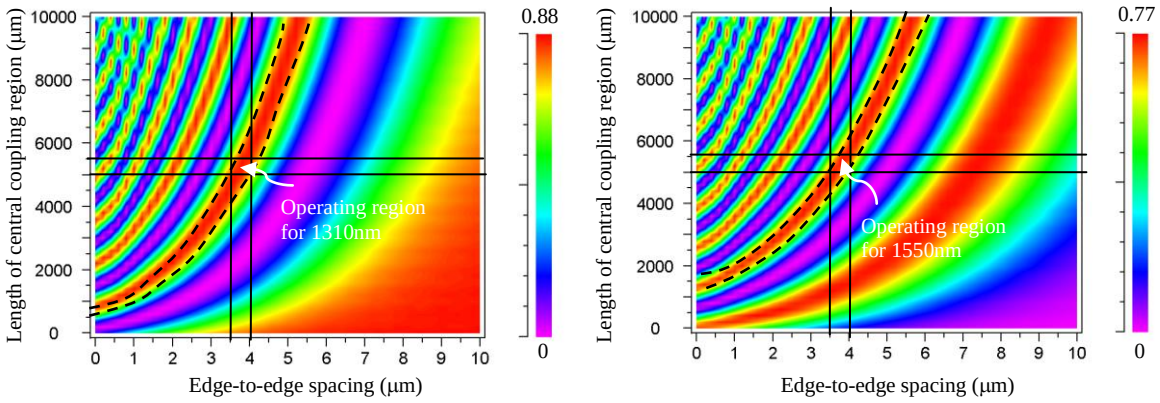

Figure 4.3: Topological charts showing the resulting power outputs for (a) 1310 nm and (b) 1550 nm wavelength with variation in length of central coupling region, *L* and edge-to-edge spacing, *d*.

Following the above, further optimization was concentrated on the parameters within the rectangular box. To identify the optimal edge-to-edge spacing corresponding to the allowable length of central coupling region, we performed iteration involving the coupling behaviors at fixed edge-to-edge spacing, *d* and varying length of central coupling region, *L*. The edge-to-edge spacing taken were *d* = 3.6 μm, 3.7 μm, 3.8 μm

and 3.9 μm. Figure 4.4 shows the normalized output intensity at output 1 and output 2 respectively as a function of the length of central coupling region with the above edge-to-edge spacing. Assuming that the 1310 nm signal wavelength is static as a standing wave, it can be seen that the 1550 nm signal wavelength shifts to the shorter length of central coupling region when increasing the edge-to-edge spacing. It is worth noting that at d = 3.8 μm, the normalized output intensity was synchronized for a particular length of central coupling region at 1310 nm and 1550 nm signal wavelengths. As such, the optimal design parameters fulfilling both power throughputs would correspond to edge-to-edge spacing, d of 3.8 μm and length of central coupling region, L of 5450 μm.

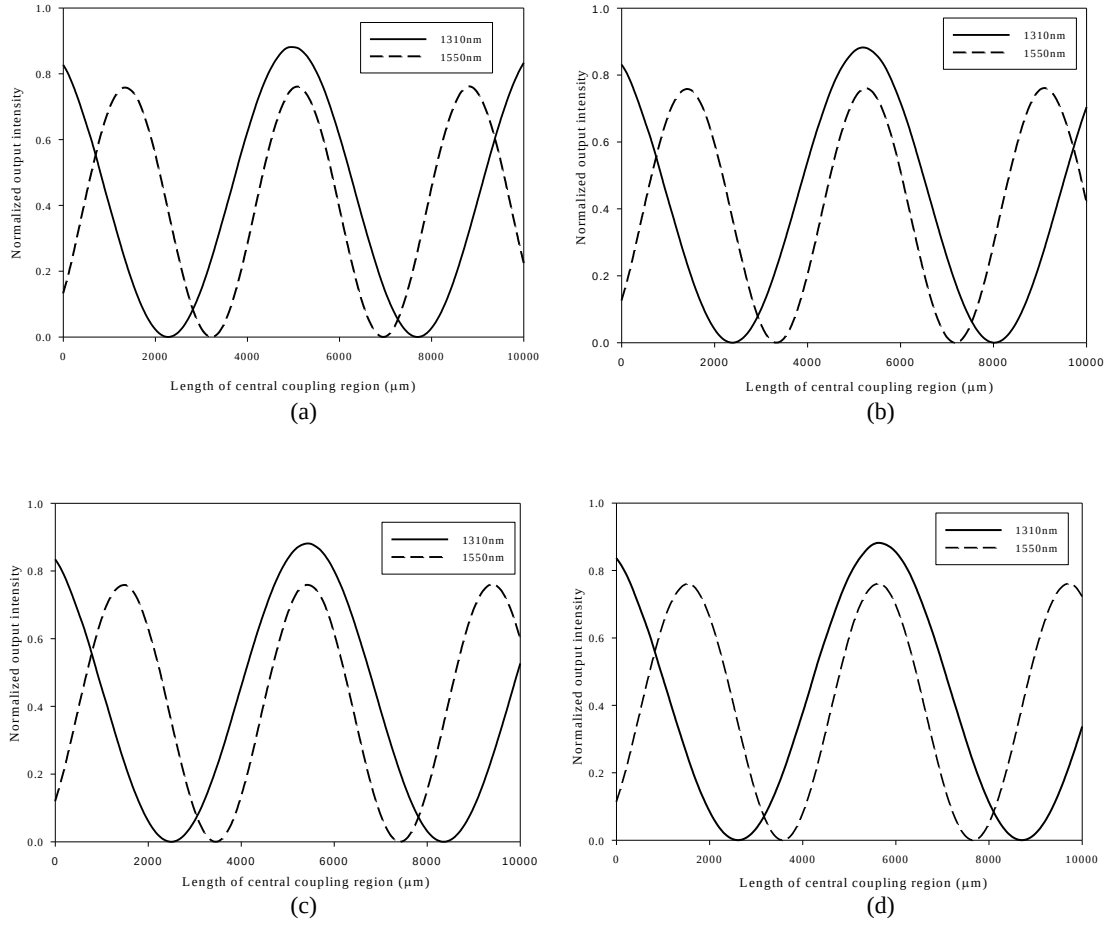

Figure 4.4: Graph showing output intensity as a function of the length of central coupling region. (Edge-to-edge separation is fixed at (a) 3.6 μm, (b) 3.7 μm, (a) 3.8 μm and (a) 3.9 μm)

Even though the power throughputs are obtained for the second 1310/1550 nm directional coupler are identical to the first 1310/1550 nm directional coupler, optimization is still needed for the second 1310/1550 nm. This is owing to the dissimilar converging arm (s-bend) with different curvature radius constructed and we believe that some additional coupling taken place between two cores along the converging arm especially at the place near to the straight coupling region. Further iteration was performed at fixed edge-to-edge spacing of 3.8 μm and varying lengths of the coupling region. The optimal length of the coupling region is reduced to 5200 μm for the second 1310/1550 nm directional coupler corresponding to the edge-to-edge spacing of 3.8 μm.

Subsequently, four directional couplers with optimal directional coupler parameters were joined together to form a silica-on-silicon hybrid pump/signal multiplexer for application in broadband amplifier. With reference to Figure 4.2, the 1310 nm and 1550 nm signal wavelengths from the input leg 1 port are de-multiplexed into output 1 and output 2, respectively. The 1550 nm signal wavelength is coupled with the 980 nm pump wavelengths which emerge from pump A and undergo amplification in erbium doped gain medium (dotted rectangular). Subsequently the 1550 nm signal is transmitted via the second 1310 / 1550 nm directional coupler and emerges from output 4. Similarly the 1310 nm signal wavelength from output 2 is coupled with the 800 nm pump wavelength from pump B and carried out amplification in bismuth doped gain medium. The signal 1310 nm then appears in output 4. Figure 4.5 (a) and Figure 4.5 (b) depict the transmission evolution along the hybrid pump/signal multiplexer for 1310 nm and 1550 nm, respectively. It is found that both signals are successfully multiplexed via the second 1310/1550 nm directional coupler and emerge from output 4.

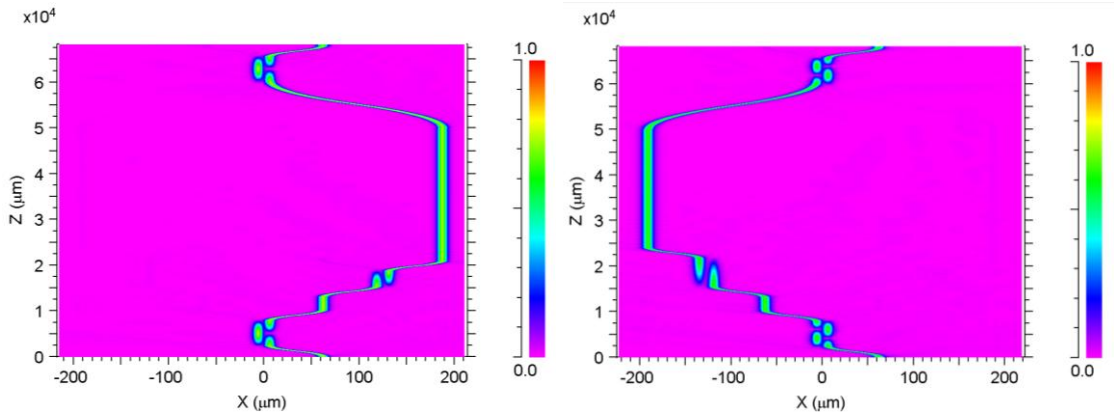

(a) 1310nm (b) 1550nm

Figure 4.5: BPM simulation showing the transmission of silica-on-silicon hybrid pump/signal multiplexer for (a) 1310 nm and (b) 1550 nm

Figures 4.5 (a) and 4.5 (b) also show that the power is almost completely transferred from input 1 to output 4 via two different paths. However, <1% residual power is transported to output 3.

The following section provides the analysis of the simulation of the silica-on-silicon hybrid pump/signal multiplexer.

4.5 Simulation Analysis of Silica-On-Silicon Hybrid Pump/Signal Multiplexer

In this section the analysis of the silica-on-silicon hybrid pump/signal multiplexer is discussed.

4.5.1 Transmission Analysis

In Figures 4.6 (a) and 4.6 (b), it can be seen that the silica-on-silicon hybrid pump/signal multiplexer suffers losses during transmission of 1310 nm and 1550 nm signal wavelengths.

Before loss compensation

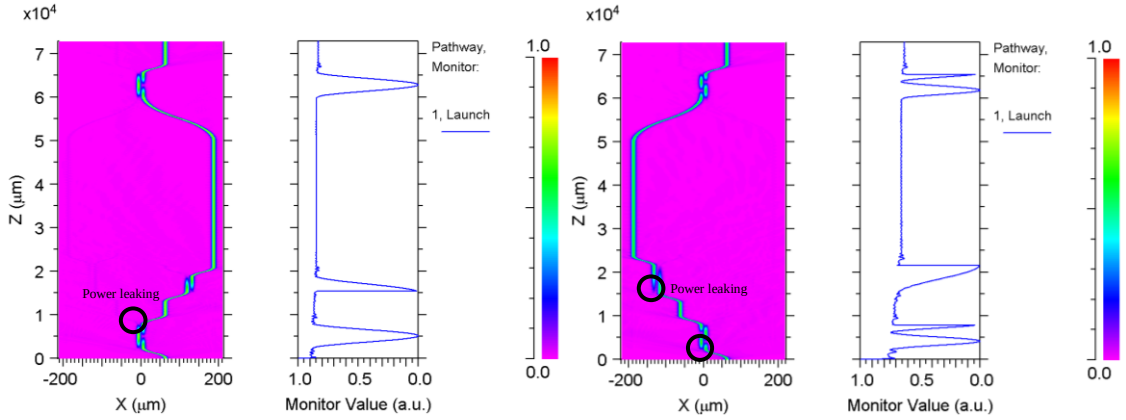

(a) 1310 nm (b) 1550 nm

After loss compensation

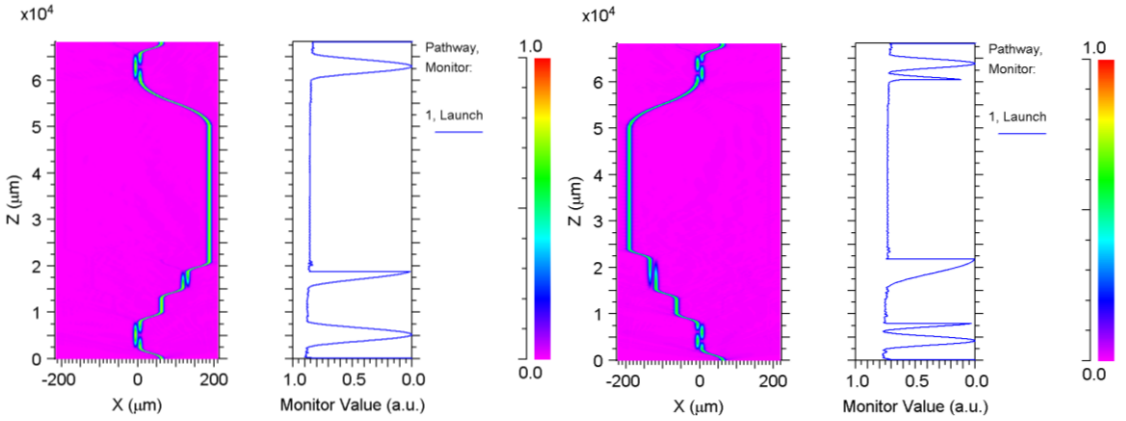

(c) 1310 nm (d) 1550 nm

Figure 4.6: BPM simulation showing the transmission of silica-on-silicon hybrid pump/signal multiplexer for (a) 1310 nm and (b) 1550 nm and their monitor values before and after loss compensation.

This can be noticed from the power monitor as depicted in Figures 4.6 (a) and 4.6 (b). Although only less than 1% of power is transmitted to the output 3, the loss is suspected to have taken place during transmission from the input to output. The loss can be calculated by using the formula for the insertion loss which is defined as the loss of signal power resulting from the insertion of a device in a planar waveguide. The insertion loss is expressed as the following:

$$\text{Insertion loss} = 10\log[P_{in} / P_{out}] \tag{4.1}$$

where P_{in} and P_{out} represent the input and output intensity respectively. Equation (4.1) takes into account only the input and output intensities. Using equation (4.1), the loss found for the transmission of 1310 nm and 1550 nm signal wavelengths are 0.24 dB and 0.87 dB, respectively. For the case of 1310 nm transmission, the 0.24 dB loss is acceptable for WDM devices, whereas the 0.87 dB is relatively high. Hence, loss compensation is necessary to carry out for the transmission of 1550 nm signal wavelengths.

The types of loss suspected to occur during transmission are the loss between two segments and bending loss. Lateral offset optimization was applied on each segment in order to reduce transmission loss between the two segments. In Figure 4.7 (a), it can be observed that the power would be leaked from the waveguide at the junction between each segment. It is attributed to the modal mismatch. The aim here is to find the optimal values of segment offset in order to maximize transmission. To do this, a series of parameters in the x-coordinates were scanned and the optimal values of segment offset were recorded. Then the device was re-simulated to validate the lateral offset optimization. Fig.4.7(c)

clears to show that the power leaking from the waveguide is much lessens and successfully improve the transmission. The values of the offset used are ranges from -0.5 μm to 0.5 μm.

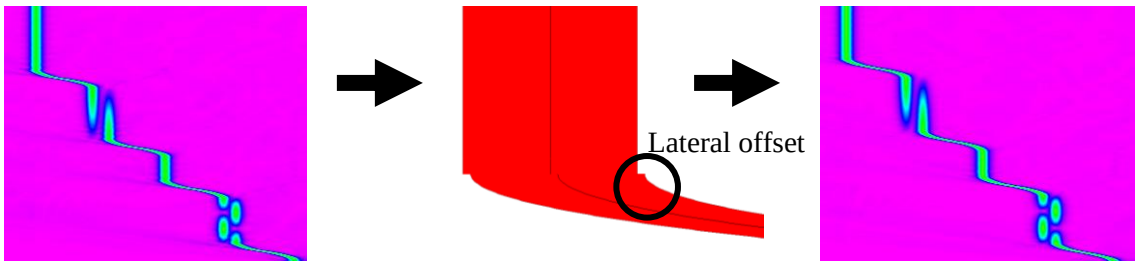

(a) (b) (c)

Figure 4.7: BPM showing the transmission evolution (a) before and (c) after the lateral offset optimization. (b) showing the lateral offset treatment.

The bend loss can be calculated using the simulated bend techniques in Rsoft BeamPROP. To do this, the mode of the bend waveguide has to be calculated first and then launched into the waveguide. A "Launch Power" monitor is set up to observe the power within the mode travelling in the waveguide. It is worth mentioning that the bending radius (R_1 = 25 mm and R_2 = 150 mm) implemented in the design is relatively large, thus the bending loss is considered negligible. Figure 4.8 illustrates the computed bending loss (fundamental mode only) for the s-bend with two different curvature radii R_1 and R_2, which are 150 mm and 25 mm, respectively. In Figure 4.8 (a) and (b), it is obvious to depict that the power drop in the bending waveguide is minimal and the power maintain at certain level with increasing the propagation length.

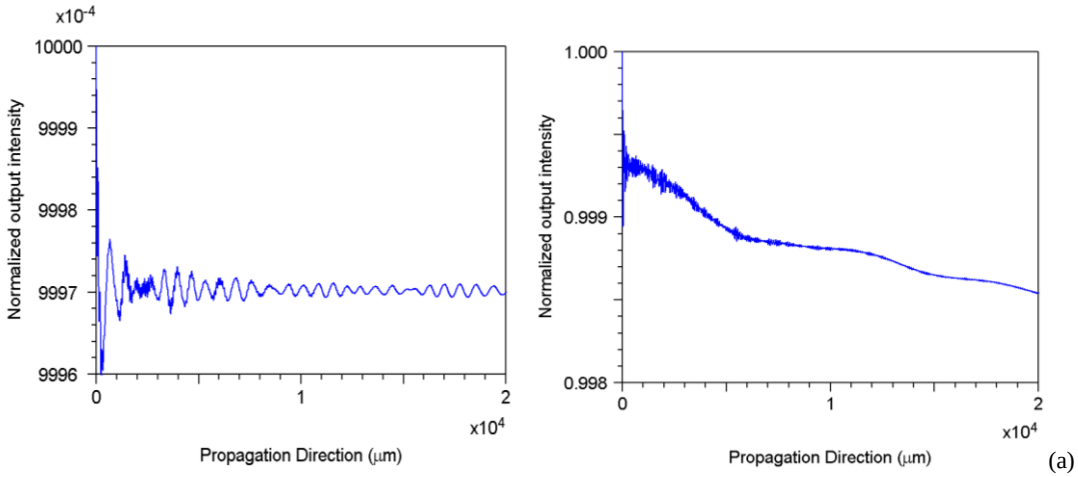

(a) R=150000μm (b) R=25000μm

Figure 4.8: The computed bending loss of fundamental mode for the s-bend with curvature radiuses R (a) 150 mm and (b) 25 mm

To this end, by reusing equation (4.1) the loss found for the transmission of 1310 nm and 1550 nm signal wavelengths are 0.23 dB and 0.33 dB, respectively after loss compensation. The power monitor and transmission evolution for 1310 nm and 1550 nm signal wavelengths are shown in Figures 4.6 (c) and (d).

4.5.2 Coupling Analysis

As already discussed in the previous chapter, all the pump and signal wavelengths mentioned in the thesis are single modal except the 800 nm pump wavelength. Besides alteration of the waveguide confinement factor, the multimodal problem can be solved by structuring a taper on the chip in order to cutoff the higher order modes. Figure 4.5 (a) shows the 1310 nm signals wavelength is almost completely transferred its energy from input 1 into output 2 and then multiplexed with 800 nm pump wavelength in 800/1310 nm directional coupler. However, there is a little power transmission in another output port. Subsequently, both signals will propagate into the bismuth doped

gain medium. Eventually, the 1310 nm signal wavelength will be coupled with 1550 nm in the second 1310/1550 nm directional coupler. Similar coupling behavior was taken place for 1550 nm signal wavelength.

4.5.3 Fabrication Tolerance Analysis

The silica-on-silicon hybrid pump/signal multiplexer design is based on the FHD thin film deposition method. Hence, the tolerance to fabrication imperfections must be considered in order to realize the devices. To maximize the tolerance from the design to fabrication, larger bandwidth or larger tolerance of the waveguide parameter is preferable. Referring back to Figure 4.3, it is shown that the region chosen for possible optimum edge-to-edge spacing and length of central coupling region have a minimal tolerance. Output results would be affected for small changing of these waveguide parameters. Figure 4.9 shows the normalized output intensity of output 4 as a function of wavelength when signal is incident through input 1.

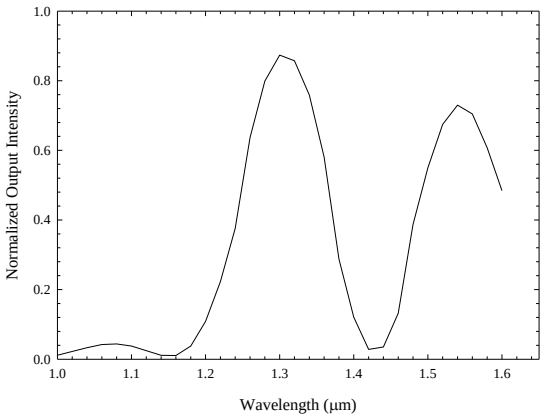

Figure 4.9: Graph showing output intensity as a function of wavelength from input 1

It can be noticed that the output intensity is not considered flatten, thus the coupling behavior is affected from different incoming signal wavelength. The device can be considered wavelength sensitive. Figure 4.10 also display the similar trend as the narrow band obtained for 1310 nm and 1550 nm signal wavelengths when varying the refractive index difference.

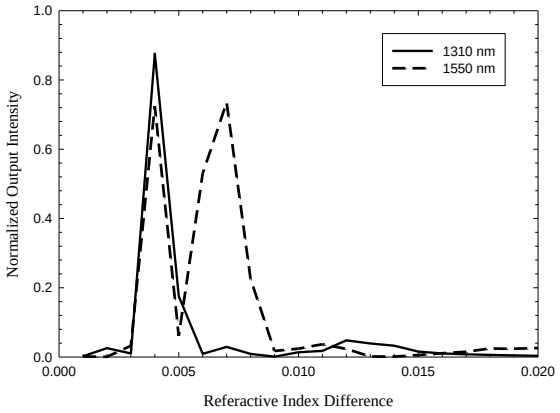

Figure 4.10: Graph showing output intensity as a function of refractive index difference for 1310 nm and 1550 nm

In conclusion, to efficiently fabricate the hybrid pump/signal multiplexer, we must have a high resolution photomask and precision etching process. Without efficient etching process, the experimental results may differ from simulation results due to small fabrication tolerance. Furthermore, refractive index control is also a critical issue in fabrication in order to obtain efficient hybrid pump/signal multiplexer.

4.6 Summary

In this chapter, a silica-on-silicon hybrid pump/signal multiplexer for application in broadband amplifier was examined. In essence, this design consists of four directional couplers and two amplifying regions. 1310 nm and 1550 nm signal wavelengths were

multiplexed and the amplifications were carried out at bismuth doped and erbium doped amplifying medium, respectively. In terms of the design, lateral offset optimization was applied in order to reduce insertion loss. The insertion loss for 1310 nm and 1550 nm signal wavelengths is 0.23 dB and 0.33 dB, respectively. From the simulation results, the contribution of bending loss on transmission is negligible. On the other hand, simulations show the process tolerances of the design are minimal. Therefore, output results would be affected for small changing of the waveguide parameters. However, this only can be validated via experimental. In summary, the advantage of the design is allowing two different telecommunication windows to carry out the amplification on the same chip in order to achieve higher capacity and bandwidth for wavelength division multiplexing (WDM) systems.

4.7 References

[1] Seo Young-Seok, Fujimoto Yasushi, Nakatsuka, Masahiro, "Optical Amplification in a Bismuth-doped Silica Glass at 1300nm Telecommunications window," Optics Communications **266**(1), 169-171 (2006).

[2] Fujimoto Y., Nakatsuka M., "Optical amplification in bismuth-doped silica glass," Applied Physics Letters **82**(19), 3325-3326 (2003).